Carpathian Journal of Earth and Environmental Sciences February 2023, Vol. 18, No. 1, p. 65 – 77; DOI:10.26471/cjees/2023/018/241

GEOCHEMICAL, MINERALOGICAL AND DIAGENETIC CHARACTERISTICS OF MARINE CHERT IN THE HATAY REGION, S-TURKEY: ITS ORIGIN AND DEPOSITIONAL ENVIRONMENT

Meryem YEŞİLOT KAPLAN[1*]

[1]Department of Petroleum and Natural Gas Engineering, Faculty of Engineering and Natural Sciences, İskenderun Technical University, Hatay, Turkey; meryem.yesilotkaplan@iste.edu.tr*

Abstract: Trace elements and rare earth elements (REEs) were studied to determine the formation of chert and siliceous limestones, which are predominantly observed in the Okçular formation. Cherts are divided into four types according to their varying forms depending on the deposition and diagenesis stages: (Type-I) layered cherts formed by direct precipitation from sea water, (Type-II) nodular cherts with rim formed by replacement, (Type-III) homogeneous chert nodules without rim, (Type-IV) chert micro nodules with high porosity. The porosity of stylolite-fracture networks and the chemical composition of seawater played a role in the formation of different types and sizes in cherts. The rim of Type II nodular cherts has significant color changes and porosity up to 20%. Anomalies of major and trace elements, especially La, Y, Sc, Ce, Th, U and Gd values, indicate direct deposition and replacement of early diagenetic pelagic deposits of cherts in the oxidized marine environment. Total (REE)+Y values, high LREE/HREE ratio and low Ce values indicate that dissolved seawater of chemical or biogenetic origin has a role in silicification. According to the similarity of the hierarchical cluster analysis of the chemical contents of the Okçular formation and the ophiolites, the silicon in the chert formation originates from the ophiolites.

Keywords: chert; rare earth elements (REEs), cluster analyses, pelagic environment, siliceous limestone

1. INTRODUCTION

Chert is a non-clastic cryptocrystalline variety of silica that occurs as nodules and horizons in limestones and sandstones. Cherts were deposited/replaced in different paleoenvironments and detailed sedimentological, stratigraphic, mineralogical, petrographic, geochemical and isotopic changes, also, the source of silica, temperature and crystallization rate or mechanisms controlling the chert formation process were investigated. The forming processes of cherts are presented under three categories: sedimentary-early diagenetic (Sharp et al., 2002; Bourli et al., 2020), diagenetic (Namy, 1974; Murray et al., 1992; Raviolo et al., 2009) and epigenetic (Kochman et al., 2020).

There are generally two models to explain the silicification stages; (1) silicification in pre-existing evaporites and/or carbonates (Bustillo, 2010) and (2) direct silica precipitation from seawater or hydrothermal fluids (Stefurak et al., 2014). Although it is observed in clastic rocks, most of the siliceous rocks are in carbonate facies (Knauth, 1992).

Elements related in silicification, especially Si, are derived from two sources: (1) they are formed by an old sea water with the effect of biogenic hydrothermal and authigenic materials, and (2) by the contribution of terrestrial material such as shale. The chemistry of a marine sedimentary rock results from: (1) the composition of the sediment; (2) components adsorbed from local seawater to grain surfaces; and (3) diagenetic process that occur during burial, lithification, and sedimentation.

Phanerozoic biogenic bedded cherts generally consist mainly of radiolaria, diatoms and/or sponge spicules (Adachi et al., 1986, Bourli et al., 2020). Radiolaria, diatoms and silica shells form the source of silica, while some internal spicules of silica contribute to silicification. Organic silica plays a role in sediments and can precipitate as cryptocrystalline, microcrystalline silica (Nichols, 2009, Liu et al., 2017). Cherts are found in sandstones and limestones as nodules and horizons. The source of silica has been associated with radiolaria, siliceous sponges and

diatoms in many studies and is therefore of organic origin. Stylolites, which are formed by intergranular solution pressure in carbonates (Ebner et al., 2010) and have different shapes and spatial distributions, can be formed due to fracture networks (Humphrey et al., 2020, Gomez-Rivas et al., 2022).

The effects of the connections, abundances and fluid flow directions of stylolite networks, which are known to have an effect on the origin studies of cherts, were investigated (Humphrey et al., 2020). Stylolites are essential for siliceous fluid movement and allow silica replacement in carbonate rocks.

The aim of this study is to interpret the local environmental characteristics, silicification source, diagenetic processes of cherts, determined by the field trip, petrographic and chemical properties and to explain the replacement story.

1.1. Geological setting

Lithostratigraphic units are widely observed in the region belongs to the Mesozoic-Quaternary period (Figures 1-2). The basement rock Kızıldağ ophiolite was placed in the region as allochthonous in the Upper Cretaceous. The Okçular formation (Middle-Upper Eocene) consists of limestone, cherty limestone and clastic limestone and all lithological units are thin-medium bedded. There are banded cherts in the Okçular formation. The Okçular formation that was deposited in a shallow marine shelf environment is overlain by the Balyatağı formation (Lower Miocene) with angular unconformity. Sofular Formation (Lower Miocene) is conformable on the underlying Balyatağı formation in Lower Miocene succession.

The Balyatağı formation sediments are fan delta deposits deposited in shallow marine and are transitional with the Sofular formation, which was also deposited in a shallow marine environment. The Tepehan formation (Middle Miocene) consisting of sandstone, clayey limestone, claystone and marl overlies the Sofular formation conformably and transitively. Quaternary alluvium, the youngest unit in the study area, overlies all units with angular unconformity.

Limestone, cherty limestone and clastic limestone are the rock types of the Okçular formation in which the cherts are found. While cherty limestones and chert bands are positioned approximately parallel to the bedding at the base, sandy limestones crop out in the limestones as lenses and intermediate levels. There are also levels consisting of reef limestones consisting of corals, components with $CaCO_3$ and fossils in the Okçular formation. Okçular formation (Lower-Middle Eocene) overlies Kaleboğazı formation (Upper Maastrichtian) with angular unconformity and the Okçular formation is very rich in macro and micro fossils.

There is lamellibranch, gastropod, echinite and coral as macrofossils in the formation. *Nummulites* cf.

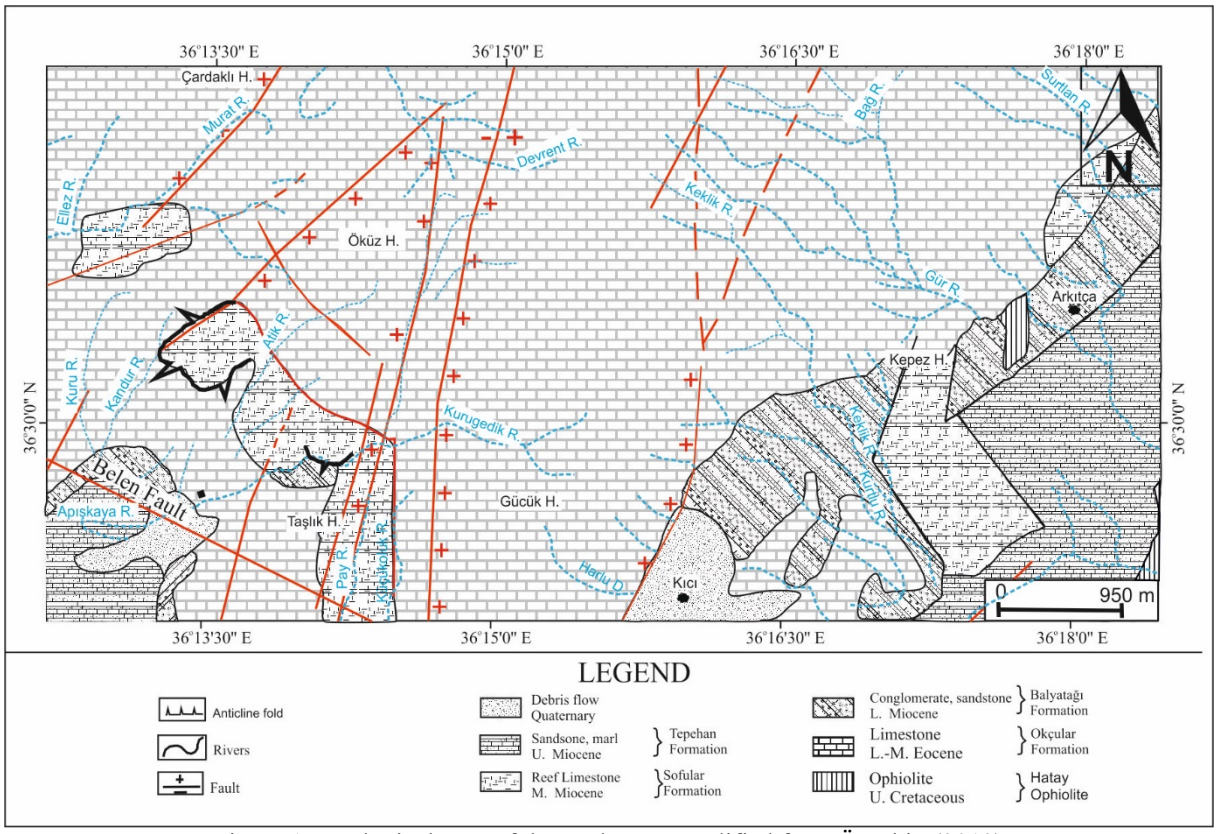

Figure 1. Geological map of the study area modified from Özşahin (2013)

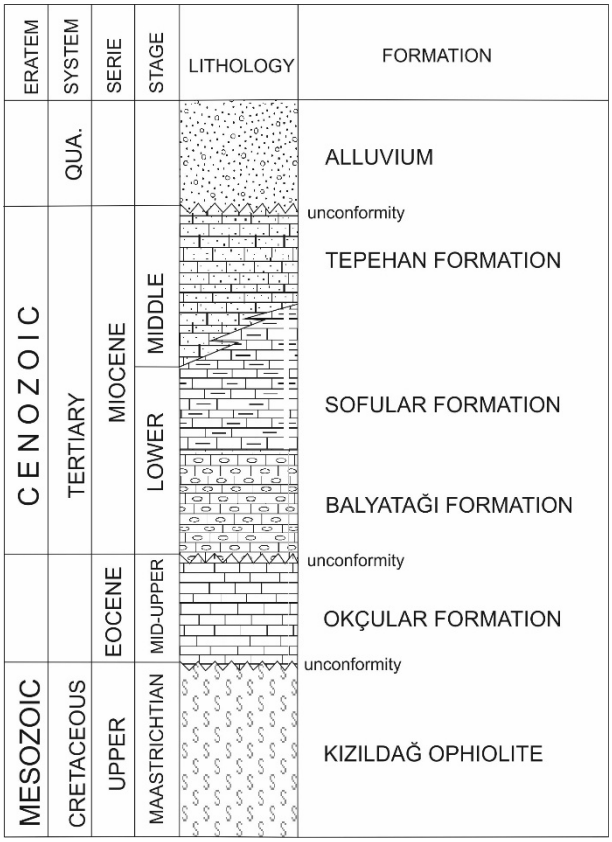

Figure 2. Generalized stratigraphic columnar sections of the Paleozoic rocks in the Belen (HATAY region)

millecaput, *Nummulites beamonti*, *Nummulites aturicus*, *Discocylina* sp., *Heterostegina* sp., *Alveolina* sp., *Alveolina fusiformis, Europertia manga, Fabiania cassis, Asterigerina rotula, Rotalia* sp., *Rotalidae, Gypsina* sp., *Assilina* sp., *Sphaerogypsina globula, Operculina* sp., *Globorotalia* sp., *Globigerina* sp., *Textularia* sp., Miliolidae and algae fossils was distinguished as microfossils from the upper levels of the unit. The formation is of Middle-Upper Lutetian-Bartonian age according to these fossils (Kavuzlu, 2006).

2. MATERIALS AND METHODS

The lithological-tectonic features of the layered, nodular chert and related lithologies were investigated, and 20 samples were taken from the bedded, nodular chert, cherty limestone and claystones that characterize the silicification stages. Optical microscopy method was used to determine texture, fossil and replacement properties.

ICP-OES for the determination of the main elements, and ICP-MS analyzes for the trace elements and REY elements were carried out in Çukurova University Laboratory (CUMERLAB). REE-Y values normalized with chondrite and PAAS (Post-Archean Australian Shale) values, the "N" subscript indicates values normalized with chondrite. The samples were normalized to the chondrite according to the Post Archean Australian Shale (PAAS) and Sun & McDonough (1989) in the study of Taylor & McLennan (1985).

Images were generated to identify pores in the chert rim and core and were determined with the open-source ImageJ program. Hierarchical cluster analysis results were used to determine the elemental similarities of the associated ophiolites and cherts to investigate the silica source.

3. RESULTS

3.1. Field trip description

There are chert morphologies observed as bedded (bedded; Type I) and nodular with different sizes in the Okçular formation. Nodular cherts are divided into two types according to whether they have rims or not: Type II is nodular cherts with rim, Type III is nodular cherts without rim.

Layered cherts (Type I) are 20-40 cm thick, medium bedded, fractured by tectonic cracks, and are more resistant to weathering than their lower-upper layers. Their colors vary from light gray to black from the crack and the upper and lower edges of the layer towards the center (Figure 3A).

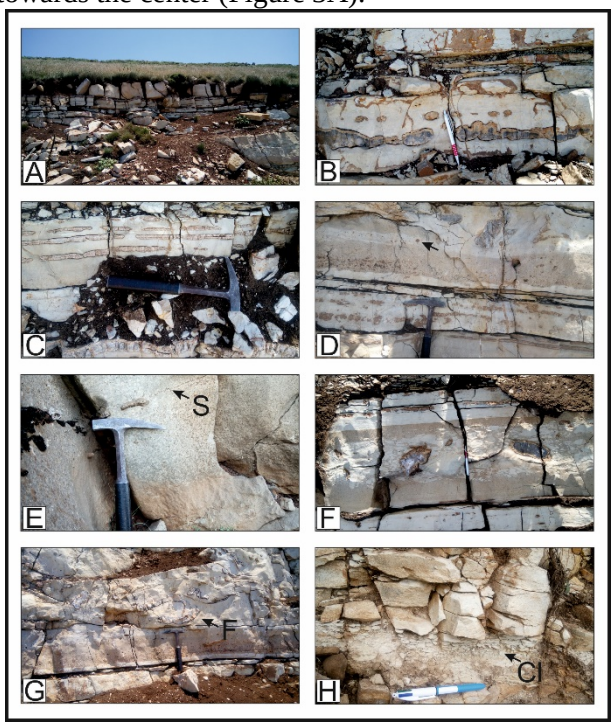

Figure 3. Field observations of cherts and associated layers (A) general view of bedded cherts, (B) general view of well-developed chert nodules with/without rim, (C) parallel chert nodules formed due to tectonic crack development, (D) Type-IV porous and brown mini cherts appearance, (E) diagenetic stylolite appearance associated with cherts, (F) tectonic fracture formed after silicification cuts into chert nodules and layers, (G) folds formed after silicification showing the

continuation of tectonic movements, (H) general view of the successive claystone layer with cherts and cherty limestones.

Chert nodules vary in color from white, brown gray to black, and their thickness varies between 1-35 cm. The chert nodules are formed singly in the cracks and their porosity changes. The nodules are of different thicknesses depending on the silica source and the abundance of addition to the environment. Parallel, thin and elongated nodules have developed with the effect of tectonic cracks (Figure 3C). Thick and well-developed chert nodules usually have a brown rim and a black center with curved edges (Figure 3B). The density of cracks is important in rim development in cherts.

Type IV usually circular nodules can reach sizes of 10-15 mm from the size of gravels. Their colors are gray and light brown, depending on the Si replacement degrees and the occurred of cryptocrystalline and they have porous textures (Figure 3D). Type IV chert nodules are scattered and observed non-parallel to the layers. The stylolites, in which the silicification fluid is transported, are concentrated where chert nodules are formed. Generally, stylolites are observed in Type IV cherts and disappear as the nodules enlarge (Figure 3E).

Tectonic cracks that play a role in the formation of chert and the presence of cracks after chert formation indicate that tectonic movements continue in the region. Figure 3F shows the fracture of chert nodules and Figure 3G shows the folding of a chert nodule/layer by tectonic movements. The Okçular formation has thin to medium bedded light gray claystone layers with a thickness of 8-35 cm, bedded with cherts, cherty limestones and limestones, overlying the chert layers and well-developed chert nodules (Figure 3H).

3.2. Petrography

Limestones with associated chert nodules and bands are in biomicritic texture and contains abundant microfossils; planktonic foraminiferas (*Morozovella* sp, *Globergerinidae, Globorotalidae*) and benthic foraminifera (including fragments of Discocyclina, Figure 4A, B). Nodular cherts were formed by the effect of replacement, with both micrite replacement and foraminiferal shell replacement in micritic limestone.

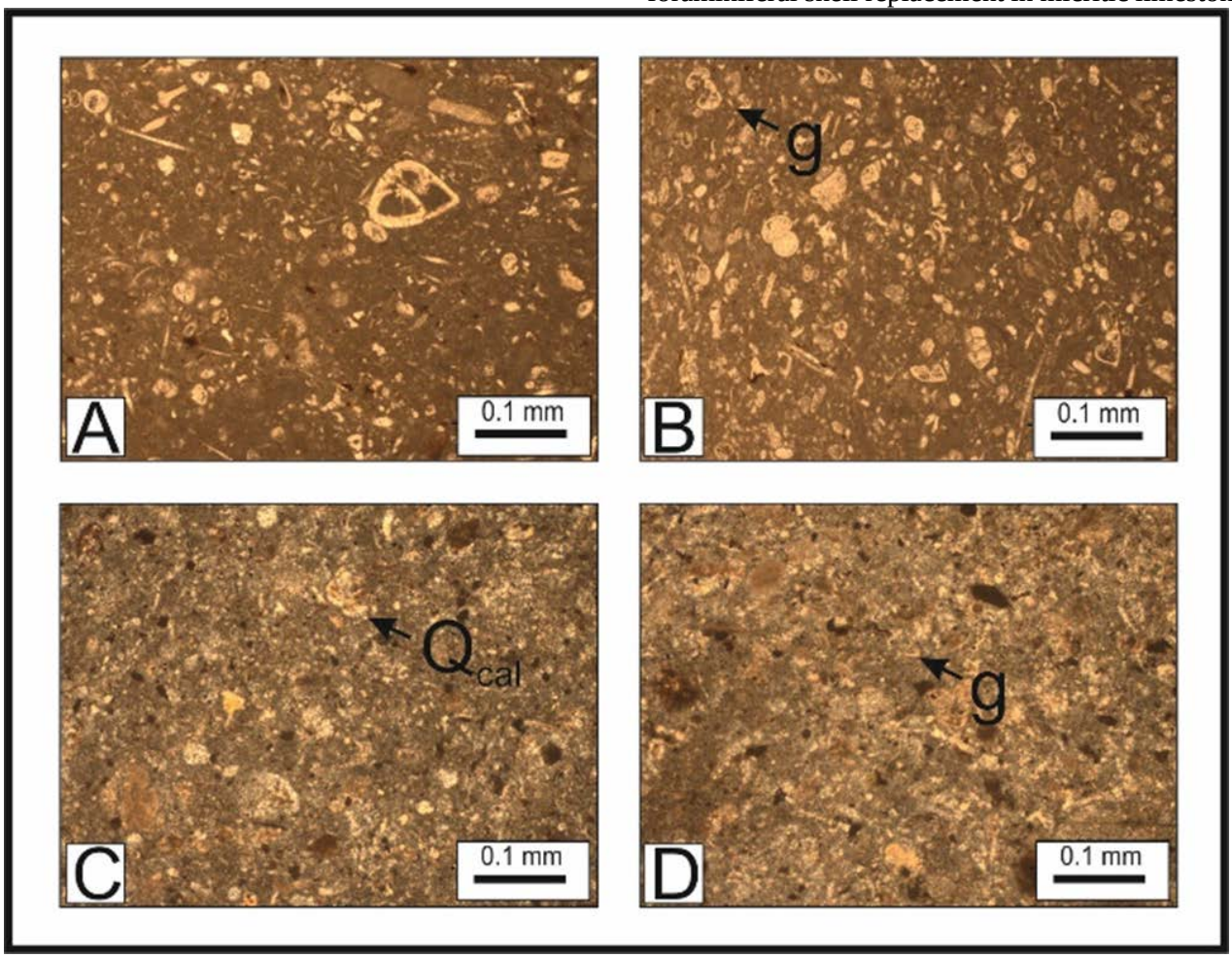

Figure 4. Petrographic images of cherts and limestones (A) Thin section view of limestone in biomicrite texture, (B) *Globigerina* (g) dominant in limestones, (C) texture preservation with silicification and coarse quartz (Q_{cal}) development in fossil shells, (D) *globotruncana* silicification

Quartz grains are clearly observed in micrite (Figures 4C, 4D). The foraminifera shells were replaced by larger silica chalcedonic crystals than the micritic material (Figure 4C). The fabric and texture protection of microfossils depends on the incomplete silicification process. Quartz crystals of approximately equal size are observed in the whole rock and they are separated by stylolites in cherts where silicification has been completed. The morphologies of some fossils were preserved in the texture where the replacement was completed and quartz crystals were dominant. Other fossils were broken and damaged (Figure 4D).

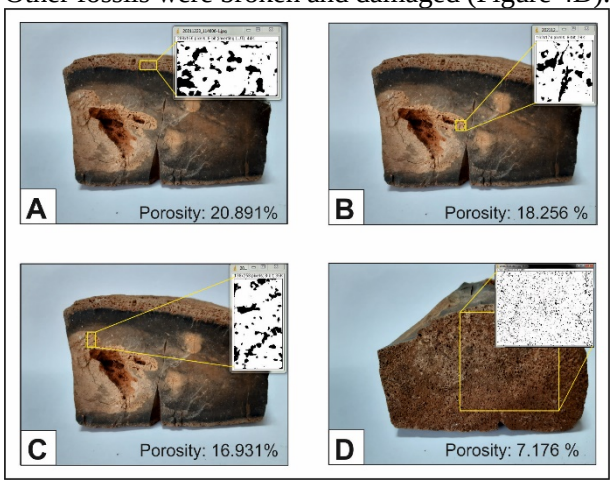

Figure 5. Zones in which pore differences due to silicification degrees were measured by image processing method in the chert nodule with rim and the measurement results.

The rim, which is more observed in nodular cherts, can be differentiated as both color and porosity changes. The porosity values observed in the core and rim of a well-developed chert nodules were measured by image processing methods. Accordingly, the observed porosity values are 20.8% in the crust and 17.6 in the center (Figure 5).

3.3. Geochemistry (Major and Trace Elements)

The main and trace (including lanthanides) elemental analyzes of cherts and cherty limestones and claystones observed in the Okçular formation are given in Table 1. In Table 2, the values calculated from the ratios of the elements are listed.

La, Pr, Nd, Ce, Eu, Sm, and Pm are light REEs (LREEs: 57-62), while Gd, Dy, Ho, Tb, Er, Yb, Tm, and Lu are heavy REEs (HREEs: 63-71). Figure 6 shows the measurement points of the samples and the REE lanthanide patterns normalized with chondrite.

3.3.1. Major Elements

Si, K, Mg, Al, Ca, Fe, Mn, Ni, Co, Zn analyzes were carried out to determine the silicification effect in cherts and their relations with the main elements and to interpret the environment. The ratios of Ca values in limestones and Si values in cherts to other main elements are higher, but it has been determined that the Si content of limestone samples in the cherts of the Okçular formation is high and therefore they are exposed to silicification with fabric-protection.

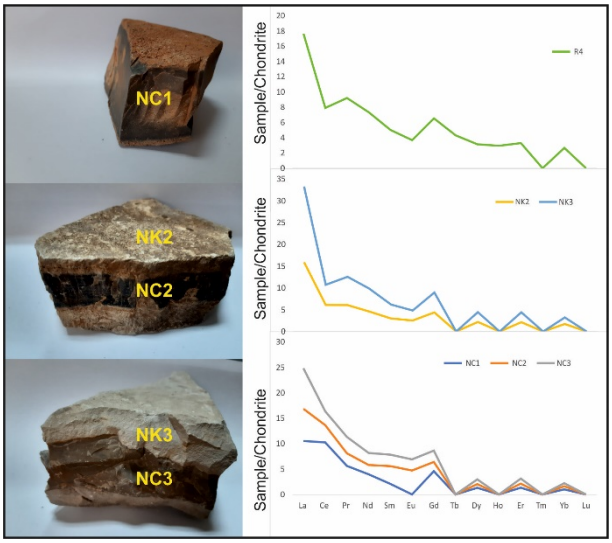

Figure 6. Sample locations of cherts (NC1-3), cherty limestones (NK2-3) and REE spider diagram of chondrite normalized Okçular formation samples

Al-Fe-Mn ternary diagrams show the contribution of hydrothermal fluids to the formation of cherts (Adachi et al., 1986; Figure 7A). If Al/(Al+Fe+Mn) values are <35, it indicates hydrothermal feeding in the environment, and an increase in this value indicates precipitation from sea water. The mean Al/(Al+Fe+Mn) value in the cherts of the Okçular Formation and the rocks associated with the cherts is 0.62, indicating the normal marine sedimentary characteristics (Webb & Kamber, 2000). Enriched redox-sensitive elements such as Ni and Co confirm the presence of anoxic and reducing conditions in the environment. These elements are absent or insignificant in the cherts of the Okçular Formation therefore the formation environment indicates oxidizing conditions. There is a negative Ce anomaly and a positive Fe-Mn minerals anomaly in seawater because tetravalent Ce is captured by Fe-Mn nodules. Cerium anomaly is negative when siliceous sediments are separated from Fe-Mn minerals (Junguo et al., 2011). Ce anomaly indicates the mixture of siliceous sediments and Fe-Mn oxides and the amount of Ce varies depending on the relevant geotectonic events.

3.3.2. Trace Elements (including REEs)

The presence of trace elements provides important environmental data in cherts, siliceous

limestones and claystones associated with cherts. Calculated values of trace elements and lanthanides used in environmental interpretations are in Table 2.

Ce concentration in shallow seawater is usually below average values (Zhang & Nozaki, 1996). The negative Ce anomaly is a typical sign of oxidized

Table 1. Major and trace (including rare elements) element geochemistry of Okçular Formation

	NC1	**NC2**	**NC3**	**NK2**	**NK3**	**R4**
Si (%)	16.20	33.43	35.20	7.39	22.68	6.15
Na (%)	0.820	0.510	0.470	0.533	0.463	0.514
K (%)	0.186	<0.02	<0.02	<0.02	0.114	<0.03
Mg (%)	0.241	0.185	0.112	0.523	0.338	1.213
Al (%)	0.504	0.359	0.282	0.426	0.287	1.628
Ca (%)	7.960	4.621	4.084	24.520	25.493	20.978
Fe (%)	0.480	0.173	0.089	0.182	0.182	1.300
Mn (%)	0.033	0.012	0.011	0.013	0.023	0.032
Ni (%)	0.002	<0.001	<0.001	<0.001	0.003	0.008
Zn (%)	0.136	0.121	0.116	0.128	0.129	0.125
Co (%)	<0.02	<0.02	<0.02	<0.02	<0.02	<0.02
La (ppm)	3.86	2.32	2.93	5.84	6.37	6.47
Ce (ppm)	9.8	3.26	2.59	5.81	4.44	7.57
Pr (ppm)	0.77	0.34	0.44	0.83	0.89	1.26
Nd (ppm)	2.82	1.3	1.68	3.26	3.74	5.21
Sm (ppm)	0.48	0.81	0.52	0.69	0.74	1.16
Eu (ppm)	<0.02	0.41	0.19	0.22	0.2	0.32
Gd (ppm)	1.4	0.56	0.68	1.34	1.4	2
Tb (ppm)	<0.01	<0.01	<0.01	<0.01	<0.01	0.25
Dy (ppm)	0.5	0.28	0.35	0.83	0.86	1.19
Ho (ppm)	<0.02	<0.02	<0.02	<0.02	<0.02	0.25
Er (ppm)	0.33	0.2	0.25	0.53	0.57	0.82
Tm (ppm)	<0.01	<0.01	<0.01	<0.01	<0.01	<0.01
Yb (ppm)	0.25	0.15	0.15	0.43	0.37	0.66
Lu (ppm)	5.019	<0.01	<0.01	<0.01	<0.01	<0.01
Sc (ppm)	281.78	272.91	237.51	253.61	246	258.41
Th (ppm)	0.46	0.39	0.45	0.26	0.23	0.78
U (ppm)	0.65	1.1	0.67	1.17	0.93	0.92
Ti (ppm)	<1	<1	<1	34.71	<1	<1
Cr (ppm)	959.5	836	762	948.74	860.32	897.62

Table 2. Calculated element values of chert and siliceous limestones of the Okçular Formation

	NC1	NC2	NC3	NK2	NK3	R4	Mean
∑REE	20.21	9.63	9.78	19.78	19.58	27.16	17.69
LREE/HREE	7.149194	7.092436	5.839161	5.319489	5.11875	4.253385	5.795403
Th/U	1.413043	2.820513	1.488889	4.5	4.043478	1.179487	2.853185
Eu/Eu*	0	1.766173	0.976418	0.686588	0.591068	0.636493	0.776123
Ce/Ce*	1.269084	0.773911	0.483483	0.552638	0.389003	0.589725	0.676307
Pr/Pr*	0.791244	0.948158	1.267124	1.13707	1.312434	1.207137	1.110528
Gd/Gd*	4.575163	0.776661	2.035087	3.463458	3.980392	1.636337	2.744516
Y/Y*	68.64	76.37143	79.95429	77.60964	81.45116	69.73445	75.62683
(La/Yb)	10.43357	10.45159	13.19964	9.177619	11.63385	6.624391	10.253441
$(La/Sm)_N$	5.061649	1.802806	3.546584	5.327331	5.418182	3.510688	4.111206
$(La/Ce)_N$	1.027087	1.855736	2.949944	2.621094	3.741126	2.228714	2.40395
$(Nd/Yb)_N$	3.934514	3.022972	3.90661	2.644425	3.525754	2.753442	3.297953
$(Dy/Yb)_N$	1.301837	1.215048	1.51881	1.256424	1.512946	1.173626	1.329782

- Ho values (≅0) are not included in the calculations

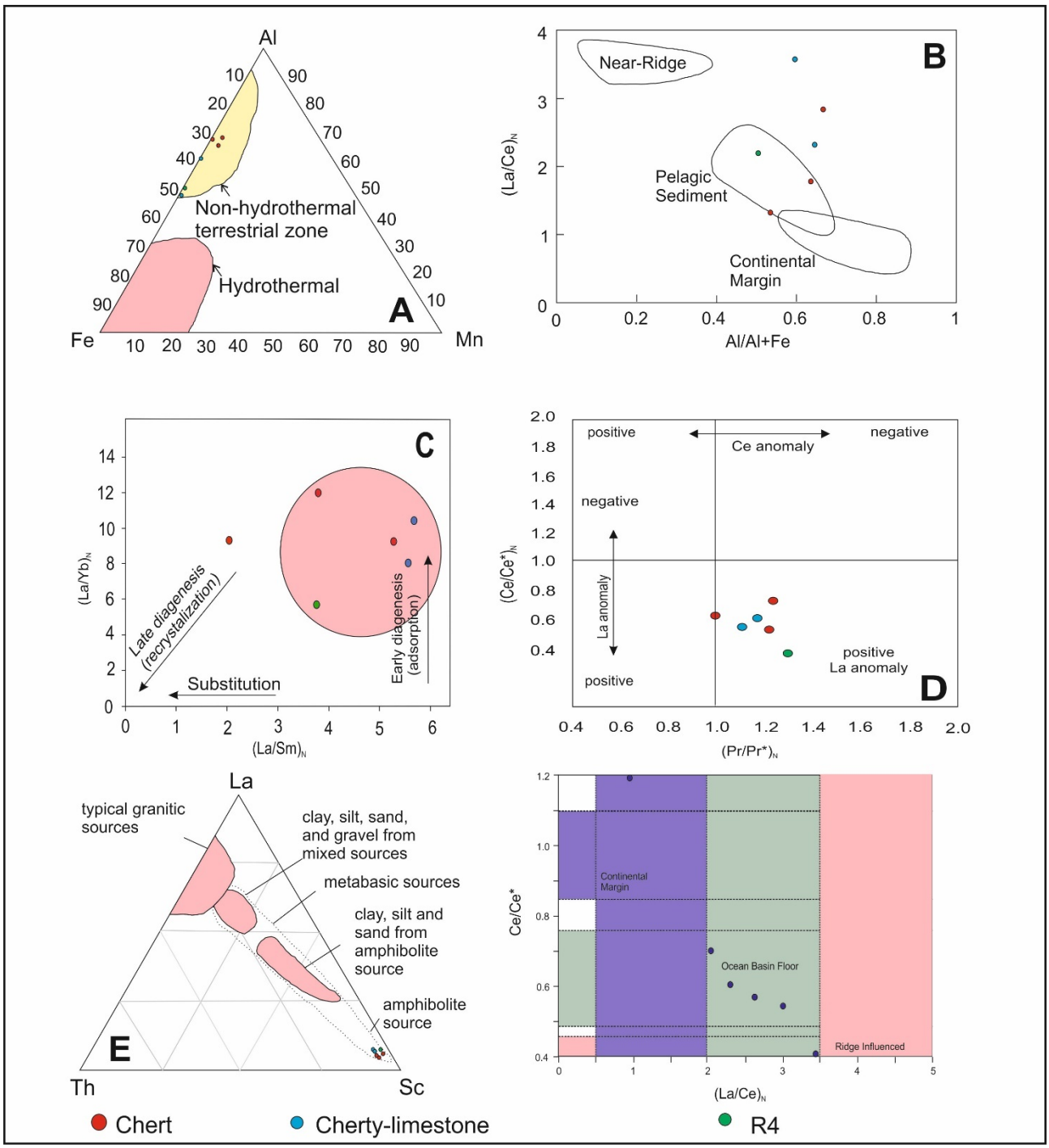

Figure 7. (A) Fe-Mn-Al ternary diagram (Adachi et al., 1986), (B) $(La/Ce)_N$ vs. Al/Al+Fe discrimination diagram for siliceous rocks, after (Murray, 1994), (C) the $(La/Sm)_N$ vs. $(La/Yb)_N$ binary plot showing the diagenesis of chert modified from Özyurt et al., 2020, (D) binary diagrams of (a) Ce/Ce * vs. Pr/Pr (Bau & Dulsky 1996), (E) Ternary plot of La-Th-Sc for cherts (F) Ce/Ce* vs. La/Ce binary diagram.

seawater (Bau & Dulski 1996; Alibo & Nozaki 1999). Ce/Ce* values are used in environmental interpretations and open ocean sea water values are between 0.2-0.3 and ~0.8-1 in continental margin deposits. Terrestrial sediment effects increase the Ce/Ce* ratio (Murray et al., 1991). Ce element indicates anoxic environment, and accordingly Ce/Ce* values are high in these environments (De Baar et al., 1988, Murray et al., 1991). The negative Ce anomaly in the REE pattern of the Okçular formation cherts is due to abrasions and oxidations (Figure 6, Kraemer et al., 2017).

Fragmentation of Gd with respect to Eu and Tb is not a redox related process because Gd is only trivalent. Differential Gd behavior relative to Eu and Tb has been documented in modern seawater and does not vary with water depth (Gd/Gd* = 1.1–2; De Baar et al., 1985). Gd_N and Eu_N anomalies were calculated as Eu/Eu* at Gd_N/Gd^* and $Eu^* = Eu_N/ (0.5Sm_N +$

$0.5Gd_N$) using Gd* = (0.5Eu + 0.5Tb) (Bau & Dulski, 1996; Nothdurft et al., 2004).

In experimental studies, it has been observed that Y, La, Gd and Lu values accumulate in solution at pH>5 (Bau, 1999). The dominant factor controlling the abnormal Gd behavior is alkalinity and carbonate complexation; however, the higher particle reactivity of Eu and Tb also influences the formation of Gd anomalies (De Baar et al., 1985). Solutions with a weak acid to near-neutral pH typically have positive Gd anomalies, while alkaline solutions have negative Gd anomalies. The absence of negative Gd in the cherts of the Okçular Formation also indicates that there is no organic complication (Lee & Byrne, 1993).

Eu (Europium) exists only in the trivalent form in sea water (Goldstein & Hemming 2014; Piper & Bau 2013). Eu complexes, like other rare earth elements, have low solubility in seawater. Eu forms (Eu^{2+} and Eu^{3+}) are controlled by oxidation-redox environments, pH and temperature. At low temperature near the surface conditions (about 25°C), Eu dominates in the trivalent state (Sverjensky, 1984). Eu^{3+} is unfractionated and stable, but Eu^{2+} dominates under extremely reducing (i.e. anoxic) alkaline conditions or high temperature (i.e. >250°C) hydrothermal conditions and fractionates according to the effect of associated REE values (Sverjensky, 1984). Therefore, positive, zero or negative Eu anomalies occur in cherts, depending on the redox, pH and temperature conditions of the precipitation. The average Eu values in the nodular and layered cherts that are the subject of the study are 0.087.

Scandium (Sc) is considered a rare earth element (REE). Scandium, a lithophile element, is the lightest of the transition elements and is found as a trace component in a wide variety of minerals, replacing Mg. Sc is usually found in clays and shales but is found in carbonates and sandstones, although relatively lower.

Sc (scandium) concentrations in surface waters are very low, usually in the range of parts per trillion (ppt). There is an average concentration of about 13 pmol L^{-1} based on limited data on Sc concentrations in seawater (Horovitz, 1999). Scandium is strongly hydrolyzed in seawater (ie $Sc(OH)^{2+}$, $Sc(OH)_3$, $Sc(OH)_4$; Byrne 2002)). Very high Sc values were measured in the lithological units of the Okçular formation, with an average of 258.41.

Continental margin environmental interpretation is made if the La/Ce ratio is <1.5 values (Murray, 1994). REE data $(La/Ce)_N$= 0.93) indicate deposition along the continental margin, further distinguishing between continental margin and pelagic deposition. It was divided into three environment according to the changes in the use of REE values and $(La/Ce)_N$ values as environment indicators; continental margin cherts (~1), pelagic cherts (2-3) and proximal ridge deposits (≥3.5) (Murray, 1994). The average $La/Ce)_N$ of 2.4 in Okçular formation cherts is the same as the values of the environment for pelagic cherts. The Ce/Ce* and $(La/Ce)_N$ values indicate the origin of the sediments, and the Ce/Ce* to $(La/Ce)_N$ diagram indicates oceanic basin floor deposits in the Okçular formation cherts (Figure 7B).

The Th/U ratio in sedimentary rocks does not show great changes depending on the deposition environment and is close to the calculated Th/U ratio in the upper continental crust (Bau & Alexander, 2009). During diagenesis and/or oxic decomposition, the Th/U ratio decreases, due to uranium oxidation (from U^{+4} to U^{+6}) (Collerson & Kamber, 1999; Bau and Alexander, 2009). Th/U values average 0.5 in Okçular Formation cherts and these low values indicate the presence of oxidation. La/Yb vs. La/Sm plots show the diagenesis process, according to which most of the Okçular formation cherts were formed from the early diagenetic stage (Fig. 7C).

If the Y/Ho ratio is <27 and the Y/Y* value is positive, the samples are super-chondritic (Gourcerol et al., 2015). Y anomalies were calculated as Y_{PAAS}/Y^* with Y* = (0.5 Dy+ 0.5 Ho) (Bau & Dulski, 2004 In references list is 1996).

Y/Ho ratios are very high (>45) in current marine waters. It is used as an indicator whether the sedimentary rocks come from sea water or clastic grains, regardless of the Y/Ho ratio. The decrease and/or depletion of the Ho element in marine environments compared to the Y element, which is similar in charge and radius, has been investigated by many studies (Bau, 1996; Van Kranendonk et al., 2003). There are studies supporting that high values do not contain marine contamination (Bau, 1999). High yttrium values were observed in other waters such as hydrothermal and magmatic waters contrary to low values in sea waters.

Nd_N/Yb_N ratios are used to determine depletion of LREEs due to the presence of positive La anomalies and negative Ce anomalies in shallow sea water (Nothdurft et al., 2004). Calculation of Ce and La anomalies are possible by comparing Pr/Pr* and Ce/Ce* ratios (Bau & Dulski, 1996). Pr/Pr* indicates >1.05 negative Ce anomaly and Ce/Ce* <1 positive La anomaly. These calculations are $Pr/Pr^* = Pr_N/ (0.5\ Ce_N + 0.5\ Nd_N)$ and $Ce/Ce^* = Ce_N/ (0.5\ La_N + 0.5\ Pr_N)$ (Table 2; Figure 7D). Okçular formation cherts have negative Ce and positive La anomaly.

The presence of combined sedimentary components in the La-Th-Sc diagram indicates that the source may be transitive. The samples are clustered in the amphibolite source in the diagram and this source originates from the Kızıldağ ophiolite which is widespread in the region (Figure 7E). The Kızıldağ

ophiolite was moved to the region as the basement rock before the Okçular formation deposition.

Yttrium (Y) is placed between Ho and Dy in the REE model according to its similar charge and radius (Bau, 1996). Figure 8 shows normalized REE patterns of elements with PAAS (Post-Archean Australian Shale) and Y anomaly in cherts. Yttrium is not removed from seawater as efficiently as its geochemical twin Ho, leading to a significant superchondritic marine Y/Ho ratio due to their different surface complex stability (Bau, 1996). Typical high Y/Ho ratios (ie 44-74) indicate seawater. The Y/Ho ratio in Okçular Formation cherts where Ho could not be detected is at its maximum value.

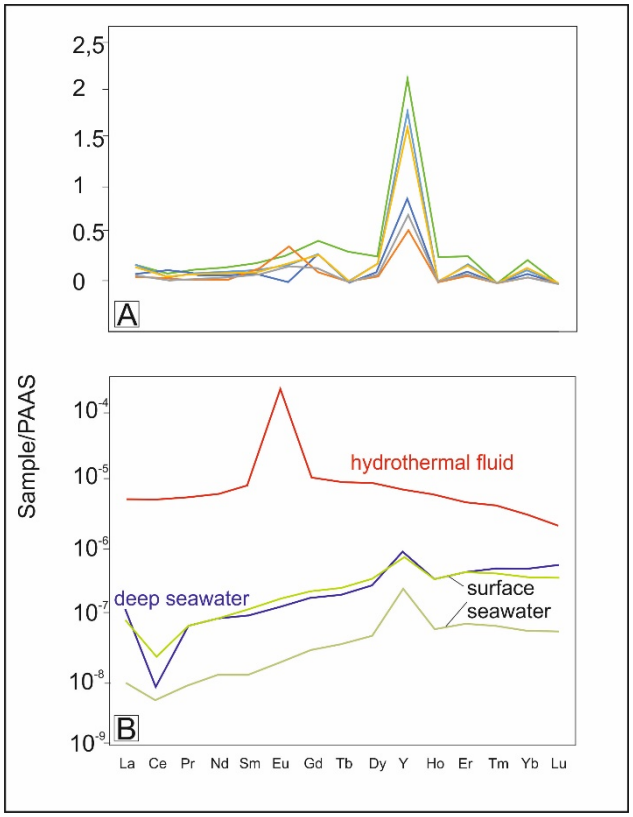

Figure 8. Comparison of REE spider diagram of PAAS normalized samples with REE patterns of shallow-deep sea and hydrothermal environments modified from He et al., (2022).

3.4. Cluster Classification

The cherts of the Okçular formation and the REE-Y cluster classifications of the ultramafic-mafic rocks were compared in order to determine the source of silicification in the region with the ultramafic-mafic rocks of the ophiolites (Figure 9). Element classifications of REE-Y values are similar in both. Tm-Lu associations were classified in both units, and the relations of HREE values were similar. Y values are classified as high and independent in both formations. Element distribution similarities show that ophiolitic rocks play a role in silicification.

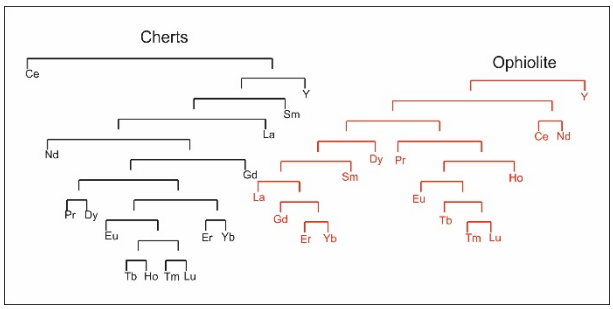

Figure 9. Cluster analyzes of element concentrations (REE+Y) in ophiolites and Okçular formation cherts and cherty limestones in Hatay region, ophiolite lanthanide values are from Güzelmansur (2020).

4. DISCUSSION

There was a regionally wide carbonate shelf in the Hatay region, on which the deposition varied between shallow sea, intertidal, and non-marine with Paleozoic development during the Late Cretaceous-Eocene periods. After the Middle Eocene (pre-Early Miocene) folding was probably caused by an early phase of continental collision that reactivated its basic structures. The Plio-Quaternary Hatay Graben was formed with the change of tectonic regime of these shallow marine carbonates after the end of Miocene (Boulton et al., 2006). Graben was formed in a transtensional environment due to the westward move of Anatolia block, and cherts are also associated with grabenization and tectonic cracks, folding and marine environments.

The presence of bedded cherts in Okçular Formation cherts, parallel to limestone bedding and laminations, is explained by the direct deposition model during lithification (Iijima et al., 1984; Raviolo et al., 2009).

Petrographic and hand specimen observations of nodular cherts show features indicating replacement. In petrographic studies, it is observed that fine-coarse quartz crystals replace calcite crystals in fractured limestones. It is probable that quartz was formed in the early diagenetic stage due to an excess of silicon, which is supported by the plot drawn with the $(La/Yb\text{-}La/Sm)_N$ values. After this stage, quartz crystallization in more porous environments indicates mid-late diagenesis (Hendry, 1995). The presence of transitions from zones with high porosity up to 21% to compact-crystalline dark colored zones in the rims and cores of nodular cherts shows the effect of pores and cracks in the replacement.

The accumulation of Fe and Mn is usually due to the effect of hydrothermal fluids, and increased Al and Ti concentrations are often due to terrestrial input to marine sediments (Murray 1994). The Al–Fe–Mn diagram is considered an indicator of the sedimentary environment (Adachi et al. 1986; Murray et al., 1991).

Okçular Formation cherts are clustered in the place representing the pelagic origin in Figure 7B diagram, and the fossil content in the limestones also indicates the pelagic origin. The Al–Fe–Mn diagram is considered an indicator of the sedimentary environment (Adachi et al. 1986; Murray et al., 1991). In Figure 7B. diagram, Okçular Formation cherts are clustered in the place representing the pelagic origin, and the fossil content in the limestones also indicates the pelagic origin. Murray (1994) stated that the Mn element will decrease in the medium with diagenetic mobility, such that the Mn values in chert samples are quite low. In addition, proximal, pelagic and continental margin environments are distinguished in the $(La/Ce)_N$-Al/Al+Fe diagram, and most of the samples point to the pelagic environment.

Many researchers have reported that the REE+Y patterns of Archaean and modern sediments are similar (Bau & Dulski, 1996; Shields & Webb, 2004; Thurston et al., 2012). The PAAS normalized Okçular formation REE-Y pattern was compared with the old marine REE patterns and both patterns were determined be similar (Figure 8). Changes in REE-Y elements also indicate precipitation from sea water. Seawater is characterized by low REE content and negative Ce anomaly, like that of the chert samples in the region (Liu et al, 2022). REE values in non-terrestrial and fine-grained clastic precipitated from seawater are used as indicators (Nothdurft et al., 2004). The sediments have a high LREE/HREE ratio because they contain more LREE precipitated from seawater due to the low rate of deposition and prolonged exposure to seawater (Murray et al., 1991). The average LREE/HREE ratio of 5.8 in Okçular Formation cherts indicates deep marine environments. LREE enrichment is determined by the $(La/Ce)_N$ ratio being close to 1 and this value is between 0.39-1.43 (avg 2.4) in this study. The $(La/Ce)_N$ mean of 2.4 also indicates pelagic cherts and indicates that silicification developed during diagenesis by being affected by siliceous fluids of pelagic mudstones.

The chondrite-normalized REE pattern of the samples is equivalent to the upper continental crust, indicating enriched LREE and depleted HREE with negative Eu anomaly. Ce-Ce* values in the Okçular formation cherts and associated rocks average 0.67 and are similar to the ocean floor values (Figure 7E). Ce/Ce* values and $(La/Ce)_N$ graphs show that the samples are affected by the source on the seafloor.

High Gd and Y values are found in the samples and low Ce and HREE values. It is available in the literature that Gd and Y values are high in oxygen-rich waters (Bau et al., 1997; Möller & Siebert, 2016). There is also this Gd and Y positive anomaly in sea waters associated with marine carbonates (Bau & Dulski, 1996). High Gd values indicate the absence of organic complexation.

Sc and Cr distributions in sediments have been proposed as indicators of detrital source (Taylor & McLennan, 1985; Condie & Wrokiewicz, 1990). The Sc values are very high in chert and siliceous limestones and represent the input of clay in the deposition and therefore the low-energy environment.

The very high Y/Ho ratio in cherts points out chert precipitation from sea water (Nozaki et al., 1997). The fact that Ho values are close to zero in Okçular Formation cherts and the observation of Y positive anomaly indicates precipitation from sea water.

Trace elements such as Th and U, which represent the ratio of felsic components in the precipitation or replacement of cherts, and trace elements such as Sc, Cr, which represent the ratio of mafic components, present wide ranges. This indicates that there are significant amounts of mafic rocks as well as felsic rocks in the source areas of the rocks.

5. CONCLUSIONS

The diversity of chert forms in the formation is seen in the excess of Si in seawater, both in direct precipitation and in replacing limestones. Fractures, porosity and tectonic movements have an effect on silicification. The characteristic REE+Y pattern, low Th/U ratio (<1), Gd, La, Y positive anomalies show that Okçular Formation carbonates and cherts precipitate from well-oxygenated seawater. It was determined that low-energy pelagic environment with trace element abundances, ophiolites are Si sources, silicification is in early-middle diagenetic stage.

REFERENCES

Adachi, M., Yamamoto, K., & Sugisaki, R., 1986. *Hydrothermal chert and associated siliceous rocks from the northern Pacific: their geological significance as indication of ocean ridge activity.* Sed Geol, 47:125–148. DOI:https://doi.org/10.1016/0037-0738(86)90075-8

Alibo, D.S., & Nozaki, Y., 1999. *Rare earth elements in seawater: particle association, shale-normalization, and Ce oxidation.* Geochimica et Cosmochimica, 63(3–4):363–372. DOI:https://doi.org/10.1016/S0016-7037(98)00279-8

Bau, M., & Dulski, P., 1996. *Distribution of yttrium and rare-earth elements in the Penge and Kuruman iron-formations, Transvaal supergroup, South Africa.* Precambr Res, 79(1–2):37–55. DOI:https://doi.org/10.1016/0301-9268(95)00087-9

Bau, M., 1996. *Controls on the fractionation of isovalent trace elements in magmatic and aqueous systems: Evidence from Y/Ho, Zr/Hf, and lanthanide tetrad effect.* Contrib. Mineral. Petrol. 123, 323–333. DOI:https://doi.org/10.1007/s004100050159

Bau, M., 1999. *Scavenging of dissolved yttrium and rare earths by precipitating iron oxyhydroxide: Experimental evidence for Ce oxidation, Y-Ho fractionation, and lanthanide tetrad effect.* Geochimica et Cosmochimica. Acta, 63, 67–77. DOI:https://doi.org/10.1016/S0016-7037(99)00014-9

Bau, M., & Alexander, B. W., 2009. *Distribution of high field strength elements (Y, Zr, REE, Hf, Ta, Th, U) in adjacent magnetite and chert bands and in reference standards FeR-3 and FeR-4 from the Temagami iron-formation, Canada, and the redox level of the Neoarchean ocean.* Precambrian Research, 174(3-4), 337-346. DOI:https://doi.org/10.1016/j.precamres.2009.08.007

Bau, M., Möller, P., & Dulski, P., 1997. *Yttrium and lanthanides in eastern Mediterranean seawater and their fractionation during redox-cycling. Mar. Chem., 56*, 123–131. DOI:https://doi.org/10.1016/S0304-4203(96)00091-6

Boulton, S.J., 2006. *Tectonic-sedimentary evolution of the Cenozoic Hatay Graben, South Central Turkey.* University of Edinburgh, unpublished PhD thesis, 414 pp.

Bourli, N., Maravelis, A. G., & Zelilidis, A., 2020. *Classification of soft-sediment deformation in carbonates based on the Lower Cretaceous Vigla Formation, Kastos, Greece.* International Journal of Earth Sciences, 109(7), 2599-2614. DOI:https://doi.org/10.1007/s00531-020-01919-4

Bustillo, M., 2010. *Silicification of continental carbonates. Carbonates in Continental Settings: Geochemistry, Diagenesis and Applications.* Developments in Sedimentology, 62. 153-178. DOI:https://doi.org/10.1016/S0070-4571(09)06203-7

Byrne, R.H., 2002. *Inorganic speciation of dissolved elements in seawater: the influence of pH on concentration ratios.* Geochem Trans 3(2):11–16. DOI:https://doi.org/10.1039/B109732F

Collerson, K. D., & Kamber, B. S., 1999. *Evolution of the continents and the atmosphere inferred from Th-U-Nb systematics of the depleted mantle.* Science, 283(5407), 1519-1522.

Condie, K.C., & Wrokiewicz, D.J., 1990. *The Cr/Th ratio in Precambrian pelites from the Kaapvaal Craton as an index of craton evolution.* Earth Planet. Sci. Lett. 97, 256–267. DOI:https://doi.org/10.1016/0012-821X(90)90046-Z

De Baar, H. J., Brewer, P. G., & Bacon, M. P., 1985. *Anomalies in rare earth distributions in seawater: Gd and Tb.* Geochimica et Cosmochimica Acta, 49(9), 1961-1969. DOI:https://doi.org/10.1016/0016-7037(85)90090-0

De Baar, H. J., German, C. R., Elderfield, H., & Van Gaans, P., 1988. *Rare earth element distributions in anoxic waters of the Cariaco Trench.* Geochimica et Cosmochimica Acta, 52(5), 1203-1219. DOI:https://doi.org/10.1016/0016-7037(88)90275-X

Ebner, M., Piazolo, S., Renard, F., & Koehn, D., 2010, *Stylolite interfaces and surrounding matrix material: Nature and role of heterogeneities in roughness and microstructural development.* J. Struct. Geol., 32, 1070–1084. DOI:https://doi.org/10.1016/j.jsg.2010.06.014

Goldstein, S.L., & Hemming, S.R., 2014. *Long-lived isotopic tracers in oceanography, paleoceanography, and ice-sheet dynamics.* In: Holland HD, Turekian KK (eds) Treatise on geochemistry, vol 8, 2nd edn. Elsevier, Amsterdam/Oxford/Waltham, pp 453–483.DOI:10.1016/B0-08-043751-6/06179-X

Gomez-Rivas, E., Martín-Martín, J. D., Bons, P. D., Koehn, D., Griera, A., Travé, A., & Neilson, J., 2022. *Stylolites and stylolite networks as primary controls on the geometry and distribution of carbonate diagenetic alterations.* Marine and Petroleum Geology, 136, 105444. DOI:https://doi.org/10.1016/j.marpetgeo.2021.105444

Gourcerol, B., Thurston, P. C., Kontak, D. J., & Côté-Mantha, O., 2015. *Interpretations and implications of LA ICP-MS analysis of chert for the origin of geochemical signatures in banded iron formations (BIFs) from the Meadowbank gold deposit, Western Churchill Province, Nunavut.* Chemical Geology, 410, 89-107. DOI: https://doi.org/10.1016/j.chemgeo.2015.06.008

Güzelmansur, Z., 2020. Kızıldağ ofiyoliti volkanik kayaçların petrografisi ve jeokimyası, Master thesis, Mersin University Institu of Science, 59 p.

He, S., Xia, Y., Xiao, J., Gregory, D., Xie, Z., Tan, Q., Yang, H., Guo, H., Wu, S., & Gong, X., *Geochemistry of REY-Enriched Phosphorites in Zhijin Region, Guizhou Province, SW China: Insight into the Origin of REY.* Minerals, 2022, 12(4), 408. DOI:https://doi.org/10.3390/min12040408

Hendry, J. P., & Trewin, N. H., 1995. *Authigenic quartz microfabrics in Cretaceous turbidites; evidence for silica transformation processes in sandstones.* Journal of Sedimentary Research, 65(2a), 380-392. DOI:https://doi.org/10.1306/D42680CC-2B26-11D7-8648000102C1865D

Horovitz, C. T., 1999. *Interactions of Scandium and Yttrium with Molecules of Biological Interest. In Biochemistry of Scandium and Yttrium*. Part 1*:* Physical and Chemical Fundamentals (pp. 235-308). Springer, Boston. DOI:10.1007/978-1-4615-4313-8_6

Iijima, A., Matsumoto, R., & Tada, R., 1984. *Mechanism of sedimentation of rhythmically bedded chert.* Sedimentary geology, *41*(2-4), 221-233. DOI:https://doi.org/10.1016/0037-0738(84)90063-0

Humphrey, E., Gomez-Rivas, E., Neilson, J., Martín-Martín, J. D., Healy, D., Yao, S., & Bons, P. D., 2020. *Quantitative analysis of stylolite networks in different platform carbonate facies.* Marine and Petroleum Geology, 114, 104203. DOI:https://doi.org/10.1016/j.marpetgeo.2019.104203

Junguo, H., Yongzhang, Z., & Hongzhong, L., 2011. *Study on geochemical characteristics and depositional environment of Pengcuolin chert, Southern Tibet.* Journal of Geography and Geology, 3(1), 178. DOI: 10.5539/jgg.v3n1p178

Kavuzlu, M., 2006. *Altınözü (Antakya) Ve Yakın Civarının*

Tektono-Stratigrafisi, Master thesis, Çukurova University Institu of Science, 82 p.

Knauth, L. P., 1992. *Origin and diagenesis of cherts: An isotopic perspective: Lecture notes in Earth Science Series.* In Isotopic signature and sedimentary records (Vol. 43) (pp. 123–152). Heidelberg: Springer-Verlag. DOI:https://doi.org/10.1007/BFb0009863

Kraemer, D., Tepe, N., Pourret, O., & Bau, M., 2017. *Negative cerium anomalies in manganese (hydr) oxide precipitates due to cerium oxidation in the presence of dissolved siderophores.* Geochimica et Cosmochimica Acta, 196,197-208. DOI:https://doi.org/10.1016/j.gca.2016.09.018

Kochman, A., Kozłowski, A., & Matyszkiewicz, J., 2020. *Epigenetic siliceous rocks from the southern part of the Kraków-Częstochowa Upland (Southern Poland) and their relation to Upper Jurassic early diagenetic chert concretions.* Sedimentary Geology, 401, 105636. DOI:https://doi.org/10.1016/j.sedgeo.2020.105636

Lee J. H., & Byrne R. H., 1993. *Complexation of trivalent rare earth elements (Ce, Eu, Gd, Tb, Yb) by carbonate ions.* Geochim Cosmochim. Acta 57, 295–302. DOI:https://doi.org/10.1016/0016-7037(93)90432-V

Liu, C., Ma, J., Zhang, L., Wang, C. & Liu, J., 2022. *Protracted formation of nodular cherts in marine platform: new insights from the Middle Permian Chihsian carbonate successions, South China.* Carbonates Evaporites 37, 15. DOI:https://doi.org/10.1007/s13146-022-00757-6

Liu, J., Ye, S., Allen Laws, E., Xue, C., Yuan, H., Ding, X., Guangming, Z., Shixiong, Y., Lei, H., Ji, W., Shaofeng, P., Yongbiao W., & Lu, Q., 2017. *Sedimentary environment evolution and biogenic silica records over 33,000 years in the Liaohe delta, China.* Limnology and Oceanography, 62(2),474-489. DOI:https://doi.org/10.1002/lno.10435

Möller, P., & Siebert, **C.**, 2016. *Cycling of calcite and hydrous metal oxides and chemical changes of major element and REE chemistry in monomictic hardwater lake; Impact on sedimentation.* Geochemistry, 76, 133–148. DOI:https://doi.org/10.1016/j.chemer.2016.01.003

Murray, R. W., 1994. *Chemical criteria to identify the depositional environment of chert: general principles and applications.* Sedimentary Geology, 90(3-4), 213-232. DOI:https://doi.org/10.1016/0037-0738(94)90039-6

Murray, R. W., Jones, D. L., & Brink, M. R. B. T., 1992. *Diagenetic formation of bedded chert: Evidence from chemistry of the chert-shale couplet.* Geology, 20(3), 271-274. DOI:https://doi.org/10.1130/0091-7613(1992)020<0271:DFOBCE>2.3.CO;2

Murray, R. W., Ten Brink, M. R. B., Gerlach, D. C., Russ III, G. P., & Jones, D. L., 1991. *Rare earth, major, and trace elements in chert from the Franciscan Complex and Montere y Group, California: assessing REE sources to fine-grained marine sediments.* Geochimica et Cosmochimica Acta, 55(7), 1875-1895. https://doi.org/10.1016/0016-7037(91)90030-9

Namy, J. N., 1974. *Early diagenetic chert in the Marble Falls Group (Pennsylvanian) of central Texas. Journal of Sedimentary Research*, 44(4), 1262-1268. DOI:https://doi.org/10.1306/212F6C8F-2B24-11D7-8648000102C1865D

Nichols, G., 2009. *Sedimentology and stratigraphy* (2nd ed.) (p. 419). Oxford: Wiley-Blackwell.

Nothdurft, L.D., Webb, G.E. & Kamber, B.S., 2004. *Rare earth element geochemistry of Late Devonian reefal carbonates, Canning Basin, Western Australia: confirmation of a seawater REE proxy in ancient limestones.* Geochim Cosmo Geochimica et Cosmochimica Acta 68(2):263–283. DOI:https://doi.org/10.1016/S0016-7037(03)00422-8

Nozaki, Y., Zhang, J., & Amakawa, H., 1997. *The fractionation between Y and Ho in the marine environment*. Earth and Planetary Science Letters, *148*(1-2), 329-340. DOI:https://doi.org/10.1016/S0012821X(97)00034-4

Özşahin, E., 2013. *Belen Tünemiş Senklinallerinin Jeomorfolojisi (Amanos Dağları, Hatay).* The Journal of Academic Social Science Studies, 6(5). DOI:http://dx.doi.org/10.9761/JASSS769

Özyurt M, Kırmacı M.Z., Al-Aasm, I., Hollis, C., Taslı, K. & Kandemir, R., 2020, *REE Characteristics of Lower Cretaceous Limestone Succession in Gümüşhane, NE Turkey: Implications for Ocean Paleoredox Conditions and Diagenetic Alteration.* Minerals,10(8):683. DOI:10.3390/min10080683

Piper, D.Z., & Bau, M., 2013. *Normalized rare earth elements in water, sediments, and wine: identifying sources and environmental redox conditions.* Am J Anal Chem 04(10):69–83. DOI:10.4236/ajac.2013.410A1009

Raviolo, M.M., Barbosa, J.A., & Neumann, V.H., 2009. *Characteristics, distribution and diagenetic stages of chert in the La Silla Formation (Lower Ordovician), Argentine Precordillera.* An Acad Bras Ciênc 81 (4):781–792. DOI:10.1590/S0001-37652009000400015

Sharp, Z. D., Durakiewicz, T., Migaszewski, Z. M., & Atudorei, V. N., 2002. *Antiphase hydrogen and oxygen isotope periodicity in chert nodules.* Geochimica et Cosmochimica Acta, 66(16), 2865-2873. DOI:https://doi.org/10.1016/j.gca.2021.11.027

Shields, G., & Webb, G., 2004. *Has the REE composition of seawater changed over geological time?* Chem. Geol. 204, 103–107. DOI:https://doi.org/10.1016/j.oregeorev.2022.105146

Stefurak, E. J., Lowe, D. R., Zentner, D., & Fischer, W. W., 2014. *Primary silica granules. A new mode of Paleoarchean sedimentation.* Geology, 42(4), 283-286. DOI:https://doi.org/10.1016/j.jseaes.2022.105143

Sun, S. S., & McDonough, W. F., 1989. *Chemical and isotopic systematics of oceanic basalts: implications for mantle composition and processes.* Geological Society, London, Special Publications, 42(1), 313-345. DOI:https://doi.org/10.1144/GSL.SP.1989.042.01.19

Sverjensky, D. A., 1984. *Europium redox equilibria in aqueous solution.* Earth and Planetary Science

Letters, 67(1), 70-78. DOI:https://doi.org/10.1016/0012-821X(84)90039-6

Taylor, S.R. & McLennan, S.M., 1985. *The Continental Crust: Its Composition and Evolution.* Blackwell, Oxford.

Thurston, P.C., Kamber, B.S., & Whitehouse, M., 2012. *Archean cherts in banded iron formation: Insight into Neoarchean ocean chemistry and depositional processes.* Precambr. Res. 214–215, 227–257. DOI:https://doi.org/10.1016/j.precamres.2012.04.004

Van Kranendonk, M. J., Webb, G. E., & Kamber, B. S., 2003. *Geological and trace element evidence for a marine sedimentary environment of deposition and biogenicity of 3.45 Ga stromatolitic carbonates in the Pilbara Craton, and support for a reducing Archaean ocean.* Geobiology, 1(2), 91-108. DOI:https://doi.org/10.1046/j.1472-4669.2003.00014.x

Webb, G.E., & Kamber, B.S., 2000. *Rare earth elements in Holocene reefal microbialites: new shallow seawater proxy.* Geochimica et Cosmochimica Acta 64: 1557-1565. DOI:https://doi.org/10.1016/S0016-7037(99)00400-7

Zhang J., & Nozaki Y., 1996. *Rare earth elements and yttrium in seawater: ICP-MS determinations in the East Caroline, Coral Sea, and South Fiji basins of the western South Pacific Ocean.* Geochimica et Cosmochimica. Acta 60, 4631–4644. DOI:https://doi.org/10.1016/S0016-7037(96)00276-1

Received at: 17. 10. 2022
Revised at: 14. 11. 2022
Accepted for publication at: 15. 11. 2022
Published online at: 18. 11. 2022